Chaos, Solitons and Fractals 175 (2023) 113961

Contents lists available at ScienceDirect

Chaos, Solitons and Fractals

journal homepage: www.elsevier.com/locate/chaos

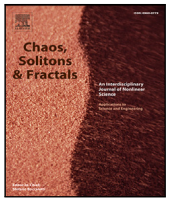

Marine ecosystem models of realistic complexity rarely exhibits significant endogenous non-stationary dynamics

Guido Occhipinti [a,b,*], Cosimo Solidoro [a,d,e], Roberto Grimaudo [c], Davide Valenti [c], Paolo Lazzari [a,d]

[a] National Institute of Oceanography and Applied Geophysics - OGS, via Beirut 2, Trieste, I-34014, Italy
[b] Dipartimento di Matematica e Geoscienze - Università degli Studi di Trieste, Via Valerio 12, Trieste, I-34127, Italy
[c] Dipartimento di Fisica e Chimica Emilio Segrè - Università degli Studi di Palermo, Viale delle Scienze, Ed. 18, Palermo, I-90128, Italy
[d] NBFC, National Biodiversity Future Center, Palermo, I-90133, Italy
[e] ICTP, International Centre Theoretical Physic , Strada Costiera, Trieste, I-34014, Italy

ARTICLE INFO

Keywords:
Ecosystem
Stability
Chaos
Biogeochemical
Lyapunov

ABSTRACT

Despite the observation of cyclic and chaotic dynamics in nature, it is still not clear whether this behaviour is inherent to ecological systems or caused by external forcings. Here we explored a set of approximately 210,000 simulations to assess how often a model of realistic complexity exhibits non-stationary dynamics when external perturbations are excluded. Remarkably, less than one third of the population shown non-stationary dynamics and, even when present, fluctuations were rather small. The inherent stability of plankton communities showed to be related to the presence of multiple feedbacks in the food web structure, omnivory, low centre of gravity, and supports the conclusion that food webs of realistic complexity rarely exhibit significant endogenous non-stationary dynamics. Finally, we computed Lyapunov exponents for the non-stationary trajectories, in order to assess in which proportion they were periodic or chaotic, and we concluded that less than 10% of the non-stationary trajectories (3% of the total) showed sensitivities to initial conditions. This further supports the conclusion that complex topology mainly damps endogenous fluctuations in the food web.

1. Introduction

Ecosystem models can exhibit stationary, cyclic, aperiodic and chaotic behaviour. Non-stationary dynamics are rather common, with examples in chemostats [1], mesocosms [2,3], and also in the acquatic ecosystems [4]. A recent meta-analysis [5] found evidence for chaos in more than 30% of time series over all organisms, and more than 50% in the plankton. Cyclic behaviour are even more common, and are discussed in any ecological textbook. However, it is still not clear whether the fluctuations observed in the field stem from a dynamics internal to the ecological system (endogenous) or are simply induced by external forcings (exogenous). Many theoretical studies highlights that simple ecological models can exhibit periodic cycles and also chaotic behaviour [6–8]. Other investigations suggest that real ecosystems are unlikely to behave chaotically unless forced by an external factor, even if their structure has the properties required (minimal complexity and presence of feedback) for doing so [9], possibly because of the presence of stabilizing regulatory processes (negative feedbacks), ubiquitous in nature, strong enough to overcompensate positive feedbacks [9].

Several studies such as [10–12] showed that long food chains are associated with greater frequency of chaos, whereas peculiar topologies of the trophic food web and the presence of certain traits, such as omnivory, can suppress chaotic behaviour. In particular, a low centre of gravity, (i.e. a high number of species near the base of the food web) inhibits chaos [10], possibly because the presence of alternative prey species for a given predator is effective in reducing unstable dynamics [10]. Similarly, the stabilizing role of omnivory, a trait often present in complex food webs in nature, has also been confirmed by field observations (see for instance [13]).

Further, analysis on simplified ecosystem models show that noise induces resonance phenomena [14]. In [15], a microcosm study was used to experimentally demonstrate that noises with characteristic time correlation properties resonate with the endogenous oscillation modes and can affect both the population dynamics and physiological behaviour. However, there is a lack of systematic studies performed with models of realistic complexity. Features such as the presence of multiple nutrients, the presence of at least several plankton populations interacting in a food web, the integration of the microbial loop, all very

* Corresponding author at: National Institute of Oceanography and Applied Geophysics - OGS, via Beirut 2, Trieste, I-34014, Italy.
E-mail address: gocchipinti@ogs.it (G. Occhipinti).

https://doi.org/10.1016/j.chaos.2023.113961
Received 27 April 2023; Received in revised form 3 August 2023; Accepted 20 August 2023
Available online 2 September 2023

common in nature and normally regarded as mandatory for realistic simulations, have not be considered yet.

The main goal of this study is to assess how frequently endogenous oscillations, or more generally non-stationary dynamics, occur in a biogeochemical model of realistic complexity, or – from another perspectives – how frequent is the stationarity in absence of external forcing.

To this aim we chose a reasonably complex state-of-the art model (BFM [16]) currently used in the European Copernicus Marine Environment Monitoring Service (CMEMS), set to constant all of its periodic external forcing and run 35000 simulations, differing for the initial conditions and the values of the model parameters (randomly perturbed), and numerically assessed the long term behaviour of each model configuration. The whole analysis was then repeated 6 times, starting from 5 different biogeochemical models, obtained by modifying the structure of BFM plankton food web. In this way we obtained 6 ensembles of 35000 simulation each, and a more general conclusion.

2. Methods

2.1. Biogeochemical processes

State of the art biogeochemical models used for ecosystem forecasting [17,18] or climate studies [19,20] are characterized by increasing complexity both in terms of number of elements fluxes across the trophic web and in terms of grazing dynamics at different trophic levels. The Biogeochemical Flux Model (BFM) [16] is a model of reasonable complexity, about 50 state variables, used for operational [21], process [22,23] and climate studies [19,24] both at the basin [22] or local [25] scales. BFM is used to model the biogeochemical component "Med-BIO" of the system "The Mediterranean Sea Monitoring and Forecasting Centre (Med-MFC)". CMEMS regularly and systematically provides key reference information on the state, variability and dynamics of the ocean, marine ecosystems and sea ice for the global ocean and the European regional seas. It was also validated against various observational reference data (satellites, literature, climatology, BGC-Argo floats) to quantify its consistency in simulating the main features of Mediterranean biogeochemistry and its accuracy in routinely reproducing the observations at specific times and locations [21]. Therefore, the BFM can be considered a state of the art model for marine biogeochemistry. BFM is formulated in terms of deterministic ordinary differential equations and accounts for the major biogeochemical processes occurring in the pelagic marine ecosystems. In its standard configuration, the BFM simulates the flow of elements (carbon, nitrogen, phosphorus, oxygen, and silica) mediated by chemical and biological processes. The microbial populations responsible for these processes are classified according to predetermined functional characteristics (traits), such as light and nutrient affinities, or diet matrix. The set of functional traits characterizing each class of organisms defines a plankton functional type (PFT). In BFM the PFTs are: (i) phytoplankton (cyanobacteria and photosynthetic protists), (ii) predators (zooplankton), (iii) decomposers (bacteria). These classes are further subdivided into functional subgroups which togheter define the planktonic food web. In particular, phytoplankton is divided into four different classes, each broadly associated also to cell size (equivalent spherical diameter — ESD): diatoms (P1, ESD = 20 to 200 μm), flagellates (P2, ESD = 2–20 μm), picophytoplankton (P3, ESD = 0.2–2 μm) and dinoflagellates (P4, ESD > 100 μm). Heterotrophic nanoflagellates (Z6, ESD = 2 to 20 μm), microzooplankton (Z5, ESD = 20 to 200 μm) and mesoozooplankton form the predator group. Mesozooplankton is composed by omnivorous mesozooplankton (Z4, ESD = 200 μm to 3–4 cm) and carnivorous mesozooplankton (Z3, ESD = 200 μm to 3–4 cm). Aerobic and anaerobic heterotrophic bacteria (B1) transform organic matter in inorganic macro-constituents such as phosphate (PO_4) and nitrate (NO_3), and contribute to the microbial food web [26].

The numerous variables considered, i.e. chemicals and physical variables, and biological species, together with their mutual interactions, make the BFM a refined and much more realistic extension of the remarkably simpler toy models used in previous studies [14,27]. The resulting trophic web and the corresponding predator–prey links are schematized in Fig. 1.

The BFM includes physiological and morphological functional traits. In general, the morphological traits include cell size, cell shape, and coloniality [28]. In BFM, only the cell size (ESD) of each PFTs is considered and it determines the dynamics of the prey–predator interactions and grazing preferences. Phytoplankton classes are further differentiated by physiological traits related to photosynthesis and nutrient uptake. Each functional group of plankton is defined by a vector of components, one for each element or constituent relevant to physiological functions. In the case of phytoplankton, the elements are carbon, nitrogen, phosphorus, silicon, and related chlorophyll molecules containing photosynthetic pigments. The grazing dynamics are expressed as biogeochemical fluxes between preys and predators. In this work we consider a spatially homogeneous system, which is therefore described by a zero-dimensional (0-D) BFM configuration, formulated as a system of 54 ordinary nonlinear differential equations and represented by a 54-dimensional state vector (V_{bfm}). The time derivatives of a generic phytoplankton carbon component (e.g., carbon in diatom, $P1_c$) or nutrient component (e.g. nitrogen in diatom, $P1_n$) are given by:

$$\frac{\partial P1_c}{\partial t} = f_c^{gpp}(V_{bfm}) - f_c^{rsp}(V_{bfm}) - f_c^{exc}(V_{bfm}) - f_c^{prd}(V_{bfm}), \tag{1}$$

$$\frac{\partial P1_n}{\partial t} = f_n^{upt}(V_{bfm}) - f_n^{rel}(V_{bfm}) - f_n^{prd}(V_{bfm}). \tag{2}$$

The f-s are continuous functions representing the biogeochemical fluxes associated to the most important physiological processes. gpp is the gross primary production (expressed in $\mathrm{mgC\ m^{-3}\ day^{-1}}$), and represents photosynthesis (i.e., flux of inorganic CO_2 to organic compounds). Respiration (rsp) is related to the release of carbon (production of CO_2). Excretion (exc) processes are related to the cell metabolic activities and the need of balancing internal quota of carbon versus other elements. In fact, in case of phosphate and nitrate shortage gpp might produce a too high carbon to phosphorus (or carbon to nitrogen) ratio inside the organism, and in this case a proper amount of organic carbon have to be released to the environment as dissolved organic carbon (DOC). The f-s are factorized in a number of regulating functions

$$f_c^{gpp}(V_{bfm}) = r_{max} f_T(T) f_I(I) f_{nut}(V_{bfm}) P1_c, \tag{3}$$

where r_{max} is the (species specific) maximum growth rate, $f_I(I)$ is an irradiance (I) harvest factor, and $f_T(T)$ is the dependence of metabolic rates on temperature (T). f_{nut} defines the limitation to growth caused by nutrient depleted conditions. In the present study, solar irradiance and temperature are considered constant. The effects of variability of I and T on the same system is describe in more detail in [29,30] which are devoted to investigate the effects of temperature and light stochastic fluctuation, respectively, on plankton dynamics.

The equations for zooplankton are similar to those for phytoplankton. In this case, the photosynthetic growth term is replaced by the grazing term (f_{gra}). As an example, in the case of carnivorous mesozooplankton we obtain

$$\frac{\partial Z3_c}{\partial t} = f_{gra}(V_{bfm}) - f_{rsp}(V_{bfm}) - f_{rel}(V_{bfm}) - f_{prd}(V_{bfm}). \tag{4}$$

The total amount of food available to zooplankton is calculated by adding the possible prey items (see Fig. 1) weighted by the predator's food preferences. Grazing analytic form (type 2) reads [31]

$$f_{gra}(V_{bfm}) = f_T(T) r_{max} \frac{F_c}{F_c + h_z} Z3_c, \tag{5}$$

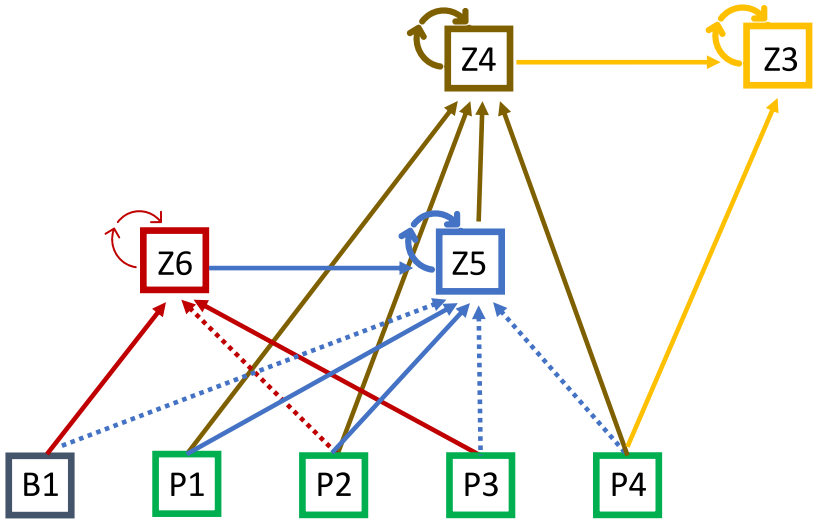

Fig. 1. Trophic web of BFM model. An arrow directed from one box to another indicates a predation flux. Solid arrows denote a higher preference for a specific prey, while dashed ones indicate a lower preference. A looping arrow on the box denotes cannibalism.

$$F_c = \sum_{prey} \delta_x e_{prey} X_i \,, \tag{6}$$

$$e_{prey} = \frac{X_i}{X_i + \mu_Z} \,, \tag{7}$$

where h_z is a parameter inversely related to the mobility and searching volume of the organism, X_i is the carbon content in the preys, δ_i is the preference for a specific prey.

The full list of equations and processes included in the BFM can be found in [22] and the BFM code manual in [16].

The deterministic configuration of the BFM model has been used in a number of studies and applications [32,21,33–39,23,40], to cite a few.

The simulations are performed solving a system of ordinary differential equations via an explicit fifth order Runge–Kutta method with adaptive time step (Python algorithm 'scipy.integrate.solve_ivp'). The results of the simulations are saved with a frequency of 1000 frames per year.

2.2. Stationarity, cycling and chaos indicators

In order to characterize the dynamic of a model trajectory we define 3 indicators. The first indicator, I_1 is the coefficient of variation (CV), to be compared to the threshold ϵ_1

$$I_1 = CV = \frac{\sigma}{\mu} \tag{8}$$

where σ is the standard deviation and μ is the mean, both computed over the time t, for $x(t)$ with t larger than t_1, and it is used to discriminate between stationary and non-stationary solutions: a trajectory is considered to be stationary if for t larger than t_1, $I_1 < \epsilon_1$, that is it fluctuates within a narrow band around μ. The second and the third indicators distinguish among the three possible non-stationary behaviours, namely a monotonic trend, a cycle, and a chaotic dynamic. In particular, the second indicator is based on the analysis of the frequency Fourier spectrum and the monotonic trajectories. Since there is always a peak at zero frequency in a Fourier spectrum due to the mean of the signal, we defined our second indicator as the ratio between the height of the second highest peak h (due to the non-stationary behaviour) and the first peak H (due to the mean),

$$I_2 = \frac{h}{H} \tag{9}$$

and defined as 'monotonic trend' the non-stationary trajectories with I_2 smaller than ϵ_2 and cyclic or chaotic the non-stationary trajectories for which $I_2 > \epsilon_2$. To avoid biased results due to the use of an automatic Python peak finder, we added the constraint that the height of the largest peak must be larger than 0.001. Also in this case the analysis is performed after a transient t larger than t_1. An example of the Fourier spectrum with peaks detected by the automatic procedure is shown in Fig. 2.

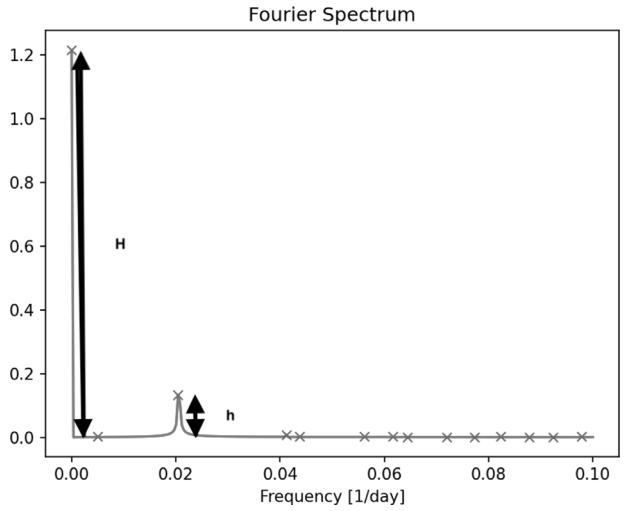

Fig. 2. Fourier transform of the zooplankton trajectory in the Rosenzweig–MacArthur model for carrying capacity $K = 2.65$. H indicates the height of the largest peak and h the height of the second largest peak. When $H > 0.001$ and $h/H > \epsilon_2$, the Fourier indicator gives a positive result.

In order to explore the robustness of our conclusion we repeated the computation of these 2 indicators using as threshold both $\epsilon_1 = \epsilon_2 = 10^{-3}$ (low threshold LT) and $\epsilon_1 = \epsilon_2 = 10^{-2}$ (high threshold HT). In all case the analysis spanned over the last 1/10 of the whole simulation ($t_1 = 9$ years)

The third indicator is related to the sensitivity to initial condition, i.e. to the presence of chaos. To determine whether a trajectory exhibits periodic or chaotic behaviour, we used the Lyapunov exponent λ (our third indicator), calculated for the last 9 years of each trajectory as in [41].

$$I_3 = \lambda \tag{10}$$

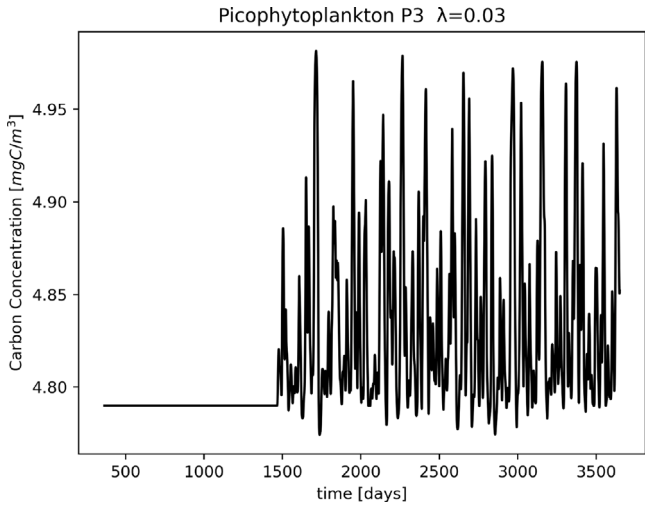

Fig. 3. A chaotic trajectory of Picophytoplankton concentration over a 9 year period, after a transient time of one year. Computed from the 0D BFM. The Lyapunov exponent is $\lambda = 0.03[d^{-1}]$, corresponding to a chaotic behaviour according to the threshold on $\lambda = 10^{-3}[d^{-1}]$.

Following the work [10], we defined as chaotic the non-stationary trajectories having I_3 greater than $\epsilon_3 = 10^{-3}[d^{-1}]$ (we consider the day length $[d]$ to be representative of the characteristic time scale of phytoplankton growth). Conversely, the periodic trajectories are those satisfying the conditions on the indicators 1 and 2 and for which $I_3 < \epsilon_3[d^{-1}]$. In Fig. 3 we show, as an example, a chaotic trajectory for the picophytoplankton group calculated with the 0D BFM and having a Lyapunov exponent $\lambda = 0.03[d^{-1}]$.

For a more comprehensive study of the biogeochemical model, we repeated the analysis with 35000 different model configurations, obtained by changing the initial conditions and the parameters of the model. The Parsac tool[1] was used to randomly perturb the model parameters (±30% with respect to their reference values [42], except for the initial conditions of nutrients, whose values were randomly sampled in the intervals $[0.01, 2.0]$ for PO_4, $[0.01, 32.0]$ for NO_3, NH_4, SiO_3, and $[5.0, 390.0]$ for dissolved oxygen). In this way we generated an ensemble of 35000 numerical realizations. Each numerical realization is run over a 10 year period, and its results are saved at a frequency of 1000 frames per year.

Due to the large number of simulations the results were analysed by aggregating the trajectories, by focusing on one parameter (p_i) at a time:

1. We subdivided the range of variation of the parameter (normally from −30% to +30% with respect to the p_i^*) in a predefined number of bins, named perturbation intervals.
2. For each perturbation interval, we classified in a set ($S^*_{I_n}$) all the simulations for which the parameter p_i belongs to the interval I_n, independently of the values of the other perturbed parameters.
3. For each S^* we counted the fraction F of stationary and non-stationary trajectories versus the total number of solutions.
4. We plotted the frequency plot of F for each perturbation interval, see Fig. 4 for an example with 4 intervals.
5. We repeated the procedure for each parameters and initial conditions.

Using the frequency plot, we can easily see if a parameter affects the stability of the ecosystem. If all the y-values of a parameter plot have the same height, the parameter has no effect, since non-stationarity occurs with the same frequency for each of its possible values (as shown in the example in panels a and c in Fig. 4); if the y-values changes, the parameter is relevant, especially for the interval of values under the highest y-values, i.e., where non-stationary solutions occur more frequently. In the example in panels b and d in Fig. 4, a non-stationary solution is more likely for higher values of the parameter p_1.

After running this extensive set of simulations derived from the nominal configuration of the BFM in the Mediterranean Sea application [21,22], we repeated the entire procedure (i.e. additional 35000 simulations and related analysis) 4 times, starting from 4 different biogeochemical models with different trophic web topologies, obtained by changing the structure of BFM plankton food-web. In particular, in addition to the full BFM, we investigated the *Long chain*, *Omn. chain*, *Omnivory*, and *Low gravity* (see Fig. 10). Bacteria were present in each configuration to preserve nutrient cycling in order to prevent the system from undergoing unrealistic temporal evolution. In each analysis we discarded the trajectories deviating from their initial food web topology due to an additional extinction occurring during the simulation.

In addition to the global variables exploration, post-processing focused on a subset of the trajectories related to the carbon concentration of the nine biological species.

2.3. Complexity and diversity

To assess the possibility of a relationship between diversity and non-stationarity, we tested the diversity index, which is a quantitative measure of how many different types (such as species) are present in a data set (community). Specifically, we used the Shannon index:

$$H = -\frac{\sum_{i=1}^{N_s} f_i \log[f_i]}{\log(N_s)}, \tag{11}$$

where N_s is the total number of species, $f_i = c_i/C_{TOT}$ is the proportion of biomass observed of a given species (c_i) divided by the total biomass concentration (C_{TOT}), log is the natural logarithm and $\log(N_s)$ a normalization factor. For example, in the BFM context, f_i is equal to the C-concentration of one of the biological species over the sum of the C-concentration of all biological species (C_{TOT}).

3. Results

The presence of periodic behaviour in ecosystems has already been explained in some situations. As an example, the widely used Rosenzweig–MacArthur model (RMA) predicts that predator–prey dynamics shift from stationarity in nutrient-poor environments to predator–prey oscillations in nutrient-rich ecosystems, and similar behaviour can be observed also in other models when the total mass of the system is increased, by increasing either the initial conditions or the nutrient input flux in a chemostat, or the carrying capacity of a system [14,43] (a two-year simulation of the RMA model is shown in Fig. 5(a)). To investigate whether a similar phenomenon can be observed in a complex biogeochemical model, we made several 10 years long BFM simulations, differing for the total mass within the system, changed by increasing the initial values of phosphate (PO_4) and nitrate (NO_3) (see Fig. 5(b) where the last two years abundances of predators and preys over the effective carrying capacity are shown). From this study it is clear that varying initial levels of nitrate and phosphate, over observable values in nature, do not lead to large fluctuations in the BFM model.

We used the set of simulations described in the previous section to examine whether the observed stationarity, Fig. 5(b), is related to the specific set of reference parameters used in BFM. In particular, we applied the aggregation procedure shown in Fig. 4 over all the parameters, and we examined further the parameter subset showing a large impact on the model stability (Fig. 6).

[1] https://github.com/BoldingBruggeman/seamless-notebooks

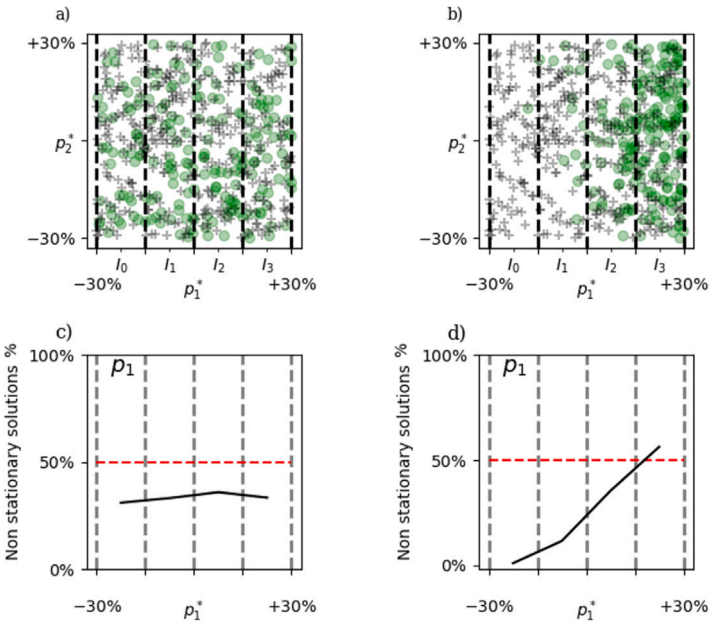

Fig. 4. Scheme illustrating the approach to analyse the occurrence of non-stationary solutions as a function of the selected parameter. We have given two example distributions, one in which the non-stationarity is distributed equally over all parameters values, the other in which the occurrence of non-stationarity is more likely for certain parameter values. In the examples shown, the system is controlled by two parameters $p_{1,2}$ with reference values $p^*_{1,2}$. The two-dimensional parameter space is divided into perturbation intervals I_0, I_1, I_2, I_3 over the axis of the selected parameter p_1 (panels a and b). Simulations with parameters p_1, p_2 leading to non-stationary solutions (green circles) and stationary solutions (grey crosses) are shown as division into slices (panels a and b). In the frequency plots of panels c and d, the corresponding fraction F of the non-stationary solutions in the total ones, as a function of the variability of p_1, is shown as a solid black line (y-values referred in the text).

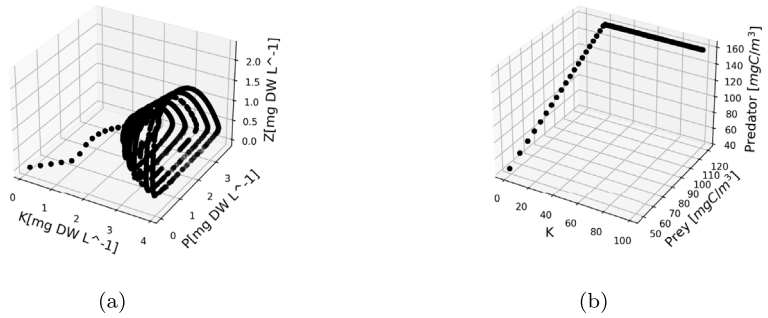

Fig. 5. (a) Rosenzweig–MacArthur model: abundances of zooplankton and phytoplankton for a 2-years period. The plot has been obtained by varying the carrying capacity K. The system displays a periodic dynamics for K greater than a certain value. (b) BFM, abundances of predators and preys for a 2-years period over the effective carrying capacity. The regime is always stationary.

We initially classified a trajectory as non-stationary using the indicators defined in the Methods section and the lower threshold (LT) of $\epsilon_1 = \epsilon_2 = 10^{-3}$ (black dashed line in Fig. 6). We adopted a biomass-based classification approach and identified a sample as non-stationary if at least one among the 9 plankton biomasses (expressed in carbon concentration) show fluctuations larger than LT, (shown in Fig. 6), as in [10]. In addition, we repeated the entire post-processing using a higher threshold (HT) for the stationarity indicators $\epsilon_1 = \epsilon_2 = 10^{-2}$ (black solid line in Fig. 6). As summarized in Table 1, the fraction of stationary trajectories increases up to 90% of the total when a less stringent threshold is adopted, i.e., when a trajectory is classified as stationary even if (slightly) larger microfluctuations are present.

An analysis of the most common model configurations leading to non-stationarity revealed that the most important parameter is the initial value of phosphate concentration (PO_4). Low initial values of this biogeochemical variable are more likely to result in non-stationarity. However the variation of the initial PO_4 concentration alone is not sufficient to induce instabilities in the BFM. Over 2500 samples where only the initial phosphate concentration was perturbed, no one exhibited cycling or chaos, consistently with the preliminary analysis shown in Fig. 5(b).

Table 1
Probability of the model to be non-stationary for two different values of threshold ϵ of the stationarity indicators.

ϵ	Non-stationary
10^{-2}	10.5%
10^{-3}	31.8%

The other nutrients, nitrate (NO_3) and ammonium (NH_4) are substitutable resources sensu Tilman [44] and an eventual unavailability of one of them is compensated by the presence of the other. Thus, to reproduce a behaviour similar to that of phosphate, we held the sum of the two nutrients "constant", obtaining the frequency plot shown in the last box of Fig. 6 ($NO_3 + NH_4$ panel).

We observe that a low initial concentration of combined nitrate and ammonium has an opposite effect to that of phosphate in the unstable behaviour when using the general condition on classification (Fig. 6), i.e., a low initial level of nutrients tends to suppress the non-stationary behaviour. Anyway for the HT the level of initial nitrate and ammonium is no longer relevant in both the cases, hence we

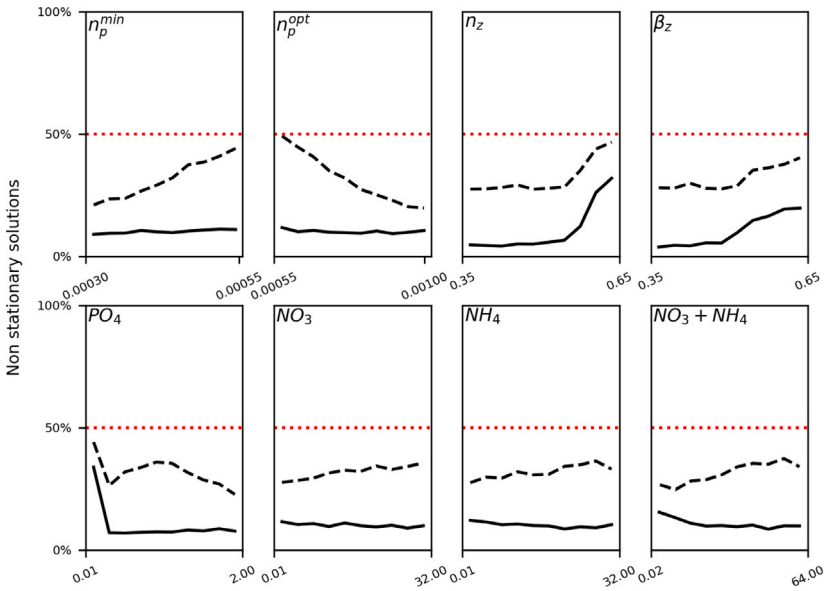

Fig. 6. Frequency plots, showing the occurrence of non-stationarities, obtained by using the biomass-based classification approach. The procedure is explained in the Methods section. For all plots, the y-axis scale is set to the interval $[0\%, 100\%]$. For the upper line of plots the x-axis limits are set to $\pm 30\%$ with respect to the reference value of the respective parameter. The x-axis is set to [0.01, 2.0] for PO_4, to [0.01, 32.0] for NO_3 and NH_4, to [0.02, 64.0] for $NO_3 + NH_4$. The black dashed line represents the SA obtained for the threshold value $\epsilon = 10^{-3}$ (LT), the black solid line for $\epsilon = 10^{-2}$ (HT). The red dotted line indicates an abundance of 50% of non-stationary solutions. Each frequency plot is constructed over 10 equal-width bins.

can discard it as an important condition for the occurrence of non-stationarities. Also the parameters n_p^{min} and n_p^{opt} are less relevant with this threshold (HT).

We investigated the role of the parameter related to the initialization of PO_4 and of two parameters (n_z and β_z) regulating the balancing flux of elements in zooplankton [eq.(2.4.4) to eq.(2.4.7) in 16]. We found that separately perturbing these parameters does not affect the stability of the model. Indeed, low values of initial PO_4 and high values of n_z and β_z lead to a remarkable change in the structure of the trophic network. In fact, under these conditions we observed an extinction of bacteria, cyanobacteria, dinoflagellates, heterotrophic nanoflagellates and carnivorous mesozooplankton, making the network more like a chain. This suggests that the topology of the network plays a role in the stability of the model, as evident in the average species distribution for stationary and non-stationary regimes, the latter characterized by a relative dominance of microzooplankton (Z5), Fig. 7.

After this preliminary SA, we focused on studying trajectories of the biomass of the nine planktonic species present in the BFM. We divided the samples into two sets: one with all non-stationary solutions, the other with stationary solutions. For these two sets of solutions, we computed the mean concentration trajectories and plotted them in Fig. 8. We can observe that also the mean non-stationary trajectories look like stationary, hence we should expect very small fluctuations around a stationary state in most of the samples.

We have already anticipated that the literature reports that complex ecological models are unlikely to exhibit non-stationary behaviour. We observed a considerable fraction of non-stationary solutions (see Table 1), but it is important to stress that such non-stationary patterns exhibit rather small perturbations (see Fig. 8). To analyse the amplitude of perturbations in the set of non-stationary solutions, we examined the coefficient of variation (CV) calculated for the last two years of each trajectory. It was found that almost all the samples are characterized by a very small CV, suggesting that the majority of the identified non-stationarities presents only very small fluctuations around an equilibrium and, from an empirical point of view, can still be assigned to stationary or quasi-stationary regime. Conversely, from an analytical/theoretical perspective, the perturbation exists, but they are present only in the very peculiar form of microfluctuations. In particular, the samples, for which the biomass CV of at least one (over

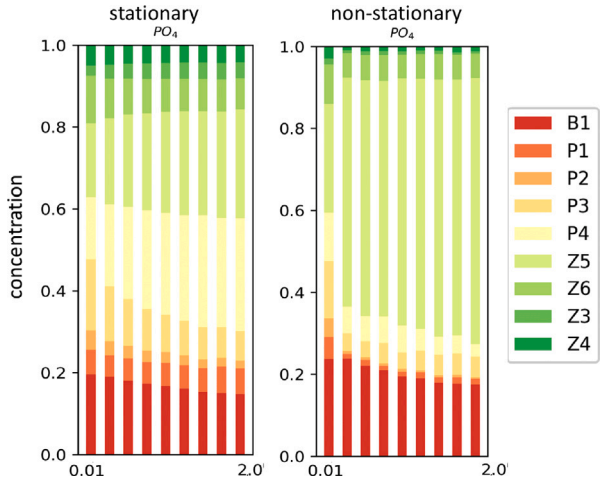

Fig. 7. Relative concentration of biological species for different values of PO_4, obtained by using the same binning as in Fig. 6, averaged over the whole stationary/non-stationary set of samples.

nine) biological species exceeds 0.05, are 10.0% of the total samples when LT is considered and 8.9% with HT. The Lyapunov exponent analysis indicates that for LT only 3.5% of the total 35000 samples contains at least one chaotic trajectory for one species biomass; for HT this resulted instead in 1.6% of the total. Therefore the relative abundance of chaotic solutions in LT and HT is approximately 10% of non-stationary ones.

To understand whether the instability, albeit small, of a complex model such as the BFM is related to the level of internal diversity of the ecosystem, we calculated the Shannon index for each sample in the stationary and non-stationary subsets and then averaged them over each subset. The non-stationary subset was identified using the HT for the indicators. The stationary and non-stationary subsets yielded mean stationary and non-stationary Shannon index equal to 0.81 and 0.56 respectively, which implies that the non-stationary behaviour is correlated to a low diversity ecosystem. Even though the diversity

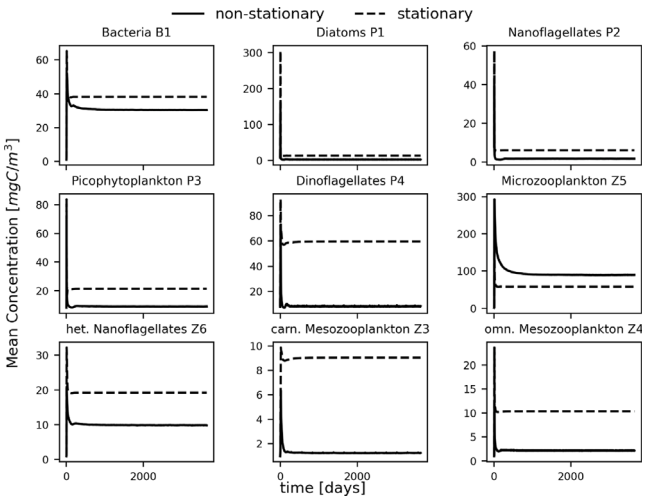

Fig. 8. Mean trajectories of the stationary samples (dashed line) and non-stationary samples (solid line) for the nine biological species of the BFM over a 10 year period. Here the threshold value $\epsilon = 10^{-2}$ (HT) is used.

index mean is lower in the non-stationary set, the distribution of the Shannon index exhibited a large spread (not shown). Therefore, we considered the Shannon index of some trajectories chosen among those which present the largest values of CV (see Fig. 10). We note that very different dynamics are characterized by similar Shannon index (0.92 and 0.90). In particular, a realization with Shannon index equal to 0.92 is characterized by fluctuations with a small amplitude (the maximum CV is 0.16; Fig. 9(a)). On the contrary, another realization with Shannon index equal to 0.90 is characterized by fluctuations with a very large amplitude (the maximum CV is 1.04; Fig. 9(b)). Further, a configuration with a small Shannon index (see Fig. 9(c)), where 6 over 9 species are close to extinction, shows fluctuations that are smaller compared to those of Fig. 9(b) (the fluctuations may even disappear with a longer simulation time), where all species are far from extinction. Finally, a configuration with an intermediate Shannon index (see Fig. 9(d)) exhibits again a dynamics different from the other cases.

It appears that non-stationary dynamics in food webs cannot be explained solely in terms of the value of the Shannon index.

Given these results, and to investigate the effects of food web topology on stationarity, we tested other four trophic web topologies in addition to the full BFM: the *Long chain*, *Omn. chain*, *Omnivory*, and *Low gravity* (see Fig. 10). Bacteria were present in each configuration to preserve nutrient cycling in order to avoid that the system can undergo an unrealistic time evolution. Analogously to what we did for the full BFM, we performed an analysis with 35000 simulations for each trophic web by perturbing the parameters and initial conditions. We used the biomass-based condition to identify a whole sample as non-stationary, with HT. In each analysis we discarded the samples deviating from their initial food web topology due to an additional extinction occurring during the simulation.

Repeating the analysis in the full BFM configuration with the above introduced constraint of preserving the trophic web topology (i.e. considering only samples without any extinction), we observed that the non-stationary sample occurrence decreases from 10.5% (see Table 1) to 2.3%

In the *Long chain* configuration, which represents a long food chain and it is analogous to the model 5A of Ref. [10], we observed an increase in the abundance (17.0%) of non-stationary samples compared to the full BFM. The configuration *Omn. chain* resulted to be similar to *Long chain* but with omnivorous species, proving to be more stable (15.9%). In the *Omnivory* configuration, with one omnivorous species (Z4) and two preys at the lower trophic level (plus bacteria), corresponding to the model 3C of Ref. [10], there is a further decrease in the occurrence (4.8%) of the non-stationary behaviour with respect to a chain structure. Finally, in the *Low gravity* configuration, characterized by a low centre of gravity (defined in Eq. (12)), i.e., a high concentration of species at the lower trophic level, and by omnivory, there are even fewer cases (3.6%) of non-stationarity.

Table 2
Probability that food webs exhibit non-stationary, periodic and chaotic dynamics. The rates were obtained over the samples that do not contain extinct species in the food web.

Food web	Non-stationary [%]	Periodic [%]	Chaotic [%]
Long chain	17.0	2.3	14.7
Omn. chain	15.9	0.0	15.9
Omnivory	4.8	1.4	3.4
Low gravity	3.6	2.5	1.1
BFM	2.3	1.6	0.7

To quantify the differences among the alternative configurations shown in Fig. 10 we considered the concept of centre of gravity of a trophic web [10] which is defined as:

$$CG := \frac{\sum_{i=1}^{N_{spec}} l_i}{N_{spec} \max_i[l_i]}, \quad 0 < CG < 1 \tag{12}$$

where l_i is the maximum chain length linking species i to basal species and N_{spec} is the number of species present in the trophic web. $CG = 0.5$ marks an unbiased distribution of species (as in all food chains), a CG greater (smaller) than 0.5 marks a concentration of species at the upper (lower) trophic levels of the web. The values of the centre of gravity of the food webs here studied are: 0.5 for *Long chain* and *Omn. chain*; 0.38 for *Omnivory*; 0.25 for *Low gravity* and BFM. In the computation of CG the bacteria were neglected. They are indeed needed for the microbial loop, but are neglected in a more idealistic representation of the food web [10].

Another indicator proposed by [10] is connectance, assuming higher connectance is related to higher stability. We computed the directed connectance [45], which also accounts for cannibalism, but it proved not to be useful. In fact the full BFM and *Low gravity* configurations had the lowest connectance, while *Omn. chain* and *Omnivory* had the highest connectance, with no clear correlation with the occurrence of non-stationarity.

Lastly, we characterized the non-stationarity as periodic or chaotic through the use of the Lyapunov exponents for each food web. The results are shown in Table 2.

4. Discussion

We have investigated the probability of obtaining non-stationary solutions in a complex ecosystem model exploring a suitably defined region of the parameter space. Several studies (e.g. [9,10]) showed that instabilities are suppressed in complex ecosystems. Therefore, we might hypothesize that the set of ensemble realizations with non-stationary behaviour are related to a reduced complexity.

To evaluate this possibility, we reduced the complexity of the BFM, by imposing extinction of some species. Specifically, we examined four configurations as well as the full BFM shown in Fig. 10 and denoted as *Long chain*, *Omn. chain*, *Omnivory*, and *Low gravity*. Two of these food web configurations, *Long chain* and *Low gravity*, were also studied in Ref. [10]. The configuration *Long chain* exhibits a larger abundance of non-stationary samples with respect to the full BFM, confirming the link between instability and a chain-like food web structure [8,10]. We found a decrease in the non-stationary behaviour in the *Omnivory* and *Low gravity* configurations. In particular, the latter configuration shows few non-stationary samples. This very stable model is characterized by a low centre of gravity and omnivory, confirming the idea that these traits are fundamental to the stability of an ecological system [10] and suggesting that the presence of alternative preys may reduce the probability of observing a non-stationary regime in ecosystems.

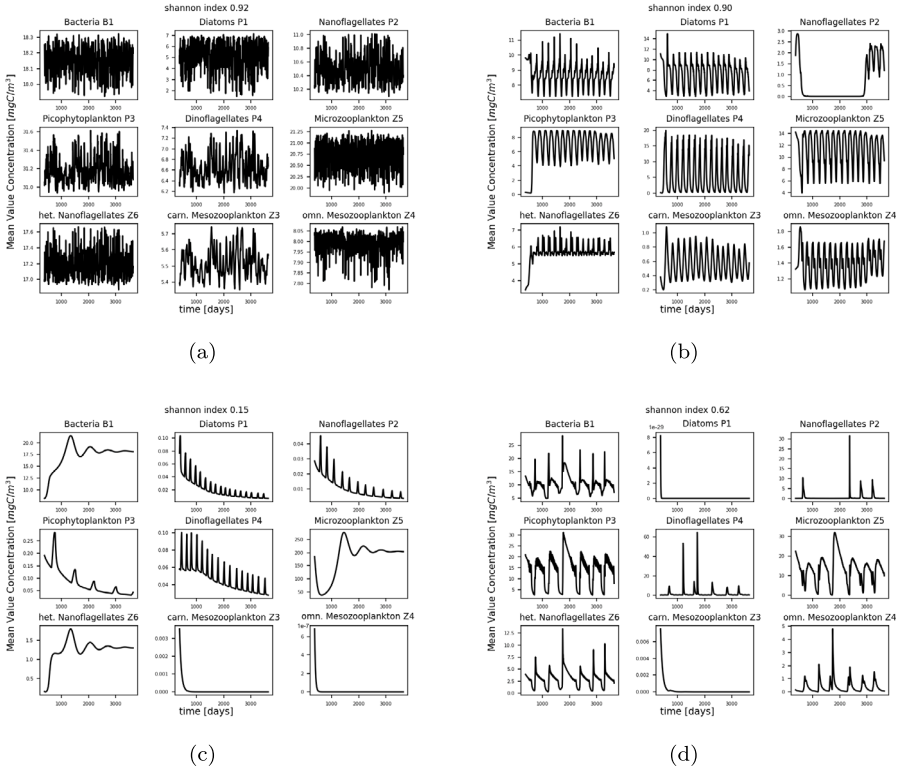

Fig. 9. Plot of non-stationary trajectories for a 10-years period, at least one trajectory for each subfigure satisfies $CV > 0.05$. The highest CV is found in: (a) Diatoms P1 with 0.16, Shannon Index 0.92; (b) Dinoflagellates P4 with $CV = 1.04$, Shannon Index 0.90; (c) Diatoms P1 with $CV = 0.27$, Shannon Index 0.15; (d) Nanoflagellates P2 with $CV = 2.75$, Shannon Index 0.62.

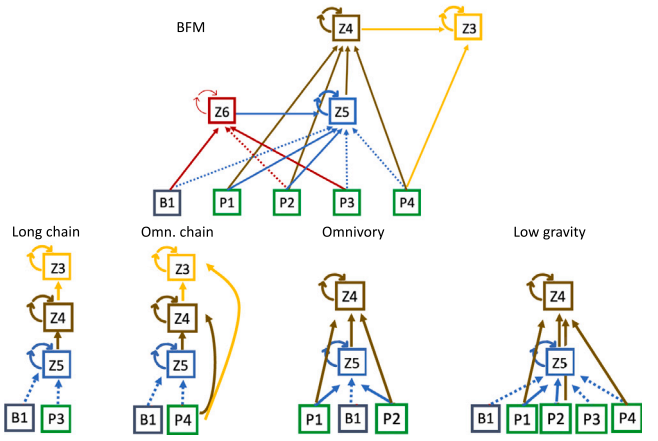

Fig. 10. Schematic representation of biological species interaction in BFM and four simplified models.

The BFM proved to be the most stable configuration, even though it has the same value of the centre of gravity as the *Low gravity* configuration. Non-stationary dynamics were observed to be less frequent in food webs with an increasing number of omnivorous links [10]. There are three omnivorous species in the BFM, but only one in the *Low gravity* configuration. This could explain the higher stability of the BFM.

The role of omnivory in food chains is still debated. It has been observed that omnivory plays a major role in stability, positive for short chains (up to three or four trophic levels), negative for longer chains [46]. In our study we found that for a four-levels omnivorous chain (with the addition of bacteria to complete the microbial loop) there was a minor decrease in the non-stationary occurrence compared to a chain of the same length without omnivores. We found only a 1% difference in the non-stationary occurrence between the *Long chain* and *Omn. chain* configurations. But we also found an increase in the occurrence of chaotic dynamics in the omnivorous chain compared to the non-omnivorous chain, so that the role of omnivory in the stability of a four-levels chain is not clear.

The frequency of chaos occurrence extends the findings of [10] and supports the conclusion that food chains are more likely to exhibit chaotic dynamics, while structural features such as a low centre of gravity may limit the occurrence of chaos.

The result that up to one third (see Table 1) of the possible parameter choices leads to microfluctuations and therefore non-stationary dynamics is consistent with the notion that complex ecological systems are in a stationary, or almost stationary, state when not subject to external forcing [9]. Thanks to the large number of different combinations of simulations (35000), we can assume that the ensemble is large enough to properly sample the sets of realistic parameter values. Moreover, the non-stationary solutions occur more frequently when the initial phosphate concentration and the two parameters (n_z and β_z), which regulate the balancing flux of elements in microzooplankton are sampled at the edges of their range of validity. Therefore, neglecting the unrealistic parametrizations, which are associated with a greater frequency of non-stationary occurrence, would increase the reliability of our conclusion: in the absence of external forcings a realistic model rarely exhibits endogenous fluctuations of significant intensity. In fact it should be noted that the threshold value $\epsilon = 10^{-3}$ (LT), and even $\epsilon = 10^{-2}$ (HT) for some variables, is below the experimental error of the biogeochemical properties taken into account. For practical reasons the HT should be considered, which significantly reduces the number of non-stationary configurations.

Ecological systems manifest positive feedback processes and over-compensatory negative feedbacks that enable the system to spend most of its time out of equilibrium [47]. Such properties are called *seeds of chaos* because, if the feedbacks are strong enough (or forced by external

factors), the system will never reach a stationary state and could behave chaotically [9].

The small perturbations we have identified as characteristic of the BFM may indeed represent the effects of feedbacks, but apparently their interactions keep the fluctuations small and the trajectory close to a stationary state. It is clear that the addition of external periodic forcing, or perhaps even just environmental noise, could modify these dynamics, and drive cyclic and chaotic behaviour in some of the trajectories currently classified as stationary [48]. However, this would be, indeed, the results of an exogenous forcing, and its interaction on exogenous dynamics, and therefore out of the scope of the present study. Surely, our study, which demonstrated the rarity of endogenous significant non-stationary behaviours in a model of realistic complexity, could evolve in future work in which a similar analysis is conducted in the presence of periodic and random environmental perturbations in the ecosystem.

5. Conclusion

The analysis of a very large number of numerical simulations performed with a marine biogeochemical model of realistic complexity highlights how in the vast majority of cases in absence of exogenous periodic forcing the system shows a stationary behaviour, therefore supporting the conclusion that the non-stationary behaviour frequently observed in nature is driven mainly by environmental forcing, such as light or temperature. The ensemble includes most – if not all – realistic model configurations. The analysis suggests that only 10% of the possible configuration exhibited – after an initial transient – fluctuations larger than 1% of a mean value, and about 1% of the total samples have chaotic trajectories.

We identified the causes of food web stability (stationarity) in topological properties of the food web, such as omnivory and a low centre of gravity, i.e., a high concentration of species in the lower trophic levels. Omnivory alone is not always sufficient to stabilize a food web: on the contrary, in long chains it plays a destabilizing role.

Our results also offer further evidence to support the conclusion that ecosystem stability is related to complex trophic food web topology, in which predators can feed on multiple preys, potentially also over multiple trophic levels, and the presence of multiple interacting feedbacks dampen fluctuations to low levels.

Code availability

The code for the BFM and its manual can be freely downloaded at bfm-community.eu. The code of the parsac tool to perform sensitivity analysis can be freely downloaded at github.com/BoldingBruggeman/seamless-notebooks. The code developed in this work to compute Lyapunov exponents and perform the stability analysis can be freely downloaded at [49].

Funding

This work was supported by OGS and CINECA under HPC-TRES program [grant number 2021-04]. GO, RG and DV acknowledge the financial support from PRIN Project PRJ-0232 - Impact of Climate Change on the biogeochemistry of Contaminants in the Mediterranean sea (ICCC). This work was partly supported by project SEAMLESS (European Union's Horizon 2020 research and innovation programme under grant agreement No 101004032). This work was partly supported by the National Biodiversity Future Center NFBC project: National Recovery and Resilience Plan (NRRP), Mission 4 Component 2 Investment 1.4 - Call for tender No. 3138 of 16 December 2021, rectified by Decree n.3175 of 18 December 2021 of Italian Ministry of University and Research funded by the European Union – NextGenerationEU.

CRediT authorship contribution statement

Guido Occhipinti: Conceptualization, Methodology, Software, Validation, Writing – original draft. **Cosimo Solidoro:** Conceptualization, Writing – original draft, Supervision, Project administration, Funding acquisition. **Roberto Grimaudo:** Conceptualization, Writing – review & editing. **Davide Valenti:** Conceptualization, Writing – review & editing. **Paolo Lazzari:** Conceptualization, Methodology, Validation, Writing – original draft, Writing – review & editing, Supervision, Project administration, Funding acquisition.

Declaration of competing interest

The authors declare that they have no known competing financial interests or personal relationships that could have appeared to influence the work reported in this paper.

Data availability

The code is shared through Zenodo, cited in the manuscript.

References

[1] Becks L, Hilker F, Malchow H, Jürgens K, Arndt H. Experimental demonstration of chaos in a microbial food web. Nature 2005;435:1226–9. http://dx.doi.org/10.1038/nature03627.

[2] Benincà E, Huisman J, Heerkloss R, Jöhnk KD, Branco P, van Nes EH, et al. Chaos in a long-term experiment with a plankton community. Nature 2008;451:822–5. http://dx.doi.org/10.1038/nature06512.

[3] Telesh I, Schubert H, Joehnk K, Heerkloss R, Schumann R, Feike M, et al. Chaos theory discloses triggers and drivers of plankton dynamics in stable environment. Sci Rep 2019;9:20351. http://dx.doi.org/10.1038/s41598-019-56851-8.

[4] Medvinsky AB, Adamovich BV, Chakraborty A, Lukyanova EV, Mikheyeva TM, Nurieva NI, et al. Chaos far away from the edge of chaos: A recurrence quantification analysis of plankton time series. Ecol Complex 2015;23:61–7. http://dx.doi.org/10.1016/j.ecocom.2015.07.001.

[5] Rogers TL, Johnson BJ, Munch SB. Chaos is not rare in natural ecosystems. Nat Ecol Evol 2022/08/01;6(8):1105–11. http://dx.doi.org/10.1038/s41559-022-01787-y.

[6] Takeuchi Y. Global dynamical properties of lotka-volterra systems. World Scientific; 1996, http://dx.doi.org/10.1142/2942.

[7] Fussmann GF, Ellner SP, Shertzer KW, Nelson G. Hairston J. Crossing the Hopf bifurcation in a live predator-prey system. Science 2000;290(5495):1358–60. http://dx.doi.org/10.1126/science.290.5495.1358.

[8] Gross T, Ebenhöh W, Feudel U. Long food chains are in general chaotic. Oikos 2005;109:135–44. http://dx.doi.org/10.1111/j.0030-1299.2005.13573.x.

[9] Berryman A, Millstein J. Are ecological systems chaotic — And if not, why not? Trends Ecol Evol 1989;4(1):26–8. http://dx.doi.org/10.1016/0169-5347(89)90014-1.

[10] Fussmann GF, Heber G. Food web complexity and chaotic population dynamics. Ecol Lett 2002;5(3):394–401. http://dx.doi.org/10.1046/j.1461-0248.2002.00329.x.

[11] Borvall C, Ebenman B, Jonsson T. Biodiversity lessens the risk of cascading extinction in model food webs. Ecol Lett 2000;3:131–6. http://dx.doi.org/10.1046/j.1461-0248.2000.00130.x.

[12] Emmerson M, Yearsley J. Weak interactions, omnivory and emergent food-web properties. Proc R Soc Lond [Biol] 2004;271(1537):397–405. http://dx.doi.org/10.1098/rspb.2003.2592.

[13] Fagan WF. Omnivory as a stabilizing feature of natural communities. Amer Nat 1997;150(5):554–67. http://dx.doi.org/10.1086/286081.

[14] Benincà E, Dakos V, Nes E, Huisman J, Scheffer M. Resonance of plankton communities with temperature fluctuations. Amer Nat 2011;178:E85–95. http://dx.doi.org/10.1086/661902.

[15] Laakso J, Löytynoja K, Kaitala V. Environmental noise and population dynamics of the ciliated protozoa Tetrahymena thermophila in aquatic microcosms. Oikos 2003;102(3):663–71. http://dx.doi.org/10.1034/j.1600-0706.2003.12319.x.

[16] M. V, T. L, M. B, L. T, P. L, G. C, et al. The biogeochemical flux model (BFM): Equation description and user manual. 2020, URL https://bfm-community.github.io/www.bfm-community.eu/files/bfm-V5.2.0-manual_r1.2_202006.pdf.

[17] Cossarini G, Feudale L, Teruzzi A, Bolzon G, Coidessa G, Solidoro C, et al. High-Resolution Reanalysis of the Mediterranean Sea Biogeochemistry (1999–2019). Front Mar Sci 2021;8:741486. http://dx.doi.org/10.3389/fmars.2021.741486, URL https://www.frontiersin.org/articles/10.3389/fmars.2021.741486/full.

[18] Skákala J, Ford D, Bruggeman J, Hull T, Kaiser J, King RR, et al. Towards a Multi-Platform Assimilative System for North Sea Biogeochemistry. J Geophys Res: Oceans 2021;126(4). http://dx.doi.org/10.1029/2020JC016649, URL https://onlinelibrary.wiley.com/doi/10.1029/2020JC016649.

[19] Solidoro C, Cossarini G, Lazzari P, Galli G, Bolzon G, Somot S, et al. Modeling carbon budgets and acidification in the Mediterranean sea ecosystem under contemporary and future climate. Front Mar Sci 2022;8. http://dx.doi.org/10.3389/fmars.2021.781522, URL https://www.frontiersin.org/articles/10.3389/fmars.2021.781522.

[20] Henson SA, Cael BB, Allen SR, Dutkiewicz S. Future phytoplankton diversity in a changing climate. Nature Commun 2021;12(1):5372. http://dx.doi.org/10.1038/s41467-021-25699-w, URL https://www.nature.com/articles/s41467-021-25699-w.

[21] Salon S, Cossarini G, Bolzon G, Feudale L, Lazzari P, Teruzzi A, et al. Novel metrics based on Biogeochemical Argo data to improve the model uncertainty evaluation of the CMEMS Mediterranean marine ecosystem forecasts. Ocean Sci 2019;15(4):997–1022. http://dx.doi.org/10.5194/os-15-997-2019, URL https://os.copernicus.org/articles/15/997/2019/.

[22] Lazzari P, Solidoro C, Ibello V, Salon S, Teruzzi A, Béranger K, et al. Seasonal and inter-annual variability of plankton chlorophyll and primary production in the Mediterranean Sea: A modelling approach. Biogeosciences 2012;9(1):217–33. http://dx.doi.org/10.5194/bg-9-217-2012, URL https://bg.copernicus.org/articles/9/217/2012/.

[23] Lazzari P, Solidoro C, Salon S, Bolzon G. Spatial variability of phosphate and nitrate in the Mediterranean Sea: A modeling approach. Deep-Sea Res I 2016;108:39–52. http://dx.doi.org/10.1016/j.dsr.2015.12.006, URL https://linkinghub.elsevier.com/retrieve/pii/S0967063715301473.

[24] Reale M, Cossarini G, Lazzari P, Lovato T, Bolzon G, Masina S, et al. Acidification, deoxygenation, and nutrient and biomass declines in a warming Mediterranean Sea. Biogeosciences 2022;19(17):4035–65. http://dx.doi.org/10.5194/bg-19-4035-2022, URL https://bg.copernicus.org/articles/19/4035/2022/.

[25] Lamon L, Rizzi J, Bonaduce A, Dubois C, Lazzari P, Ghenim L, et al. An ensemble of models for identifying climate change scenarios in the Gulf of Gabes, Tunisia. Reg Environ Change 2014;14(S1):31–40. http://dx.doi.org/10.1007/s10113-013-0430-x, URL http://link.springer.com/10.1007/s10113-013-0430-x.

[26] Legendre L, Rassoulzadegan F. Plankton and nutrient dynamics in marine waters. Ophelia 1995;41(1):153–72. http://dx.doi.org/10.1080/00785236.1995.10422042.

[27] Vilar JMG, Solé RV. Effects of Noise in Symmetric Two-Species Competition. Phys Rev Lett 1998;80(18):4099–102. http://dx.doi.org/10.1103/PhysRevLett.80.4099, URL https://link.aps.org/doi/10.1103/PhysRevLett.80.4099.

[28] Litchman E, Klausmeier CA. Trait-Based Community Ecology of Phytoplankton. Annu Rev Ecol Evol Syst 2008;39(1):615–39. http://dx.doi.org/10.1146/annurev.ecolsys.39.110707.173549, URL https://www.annualreviews.org/doi/10.1146/annurev.ecolsys.39.110707.173549.

[29] Lazzari P, Grimaudo R, Solidoro C, Valenti D. Stochastic 0-dimensional Biogeochemical Flux Model: Effect of temperature fluctuations on the dynamics of the biogeochemical properties in a marine ecosystem. Commun Nonlinear Sci Numer Simul 2021;103:105994. http://dx.doi.org/10.1016/j.cnsns.2021.105994, URL https://linkinghub.elsevier.com/retrieve/pii/S1007570421003063.

[30] Grimaudo R, Lazzari P, Solidoro C, Valenti D. Effects of solar irradiance noise on a complex marine trophic web. Sci Rep 2022;12(1):12163. http://dx.doi.org/10.1038/s41598-022-16236-w, URL https://www.nature.com/articles/s41598-022-16236-w.

[31] Gentleman W, Leising A, Frost B, Strom S, Murray J. Functional responses for zooplankton feeding on multiple resources: A review of assumptions and biological dynamics. Deep-Sea Res II 2003;50(22–26):2847–75. http://dx.doi.org/10.1016/j.dsr2.2003.07.001.

[32] Lazzari P, Teruzzi A, Salon S, Campagna S, Calonaci C, Colella S, et al. Pre-operational short-term forecasts for Mediterranean Sea biogeochemistry. Ocean Sci 2010. http://dx.doi.org/10.5194/os-6-25-2010, Copernicus Publications.

[33] Cossarini G, Lazzari P, Solidoro C. Spatiotemporal variability of alkalinity in the Mediterranean Sea. Biogeosciences 2015;12(6):1647–58. http://dx.doi.org/10.5194/bg-12-1647-2015, URL https://bg.copernicus.org/articles/12/1647/2015/.

[34] Lazzari P, Mattia G, Solidoro C, Salon S, Crise A, Zavatarelli M, et al. The impacts of climate change and environmental management policies on the trophic regimes in the Mediterranean Sea: Scenario analyses. J Mar Syst 2014;135:137–49. http://dx.doi.org/10.1016/j.jmarsys.2013.06.005, URL https://linkinghub.elsevier.com/retrieve/pii/S0924796313001425.

[35] Tedesco L, Vichi M, Scoccimarro E. Sea-ice algal phenology in a warmer Arctic. Sci Adv 2019;5(5):eaav4830. http://dx.doi.org/10.1126/sciadv.aav4830, URL https://advances.sciencemag.org/lookup/doi/10.1126/sciadv.aav4830.

[36] Polimene L, Pinardi N, Zavatarelli M, Colella S. The Adriatic Sea ecosystem seasonal cycle: Validation of a three-dimensional numerical model. J Geophys Res 2007;112(C3):C03S19. http://dx.doi.org/10.1029/2005JC003260, URL http://doi.wiley.com/10.1029/2005JC003260.

[37] Terzić E, Lazzari P, Organelli E, Solidoro C, Salon S, D'Ortenzio F, et al. Merging bio-optical data from Biogeochemical-Argo floats and models in marine biogeochemistry. Biogeosciences 2019;16(12):2527–42. http://dx.doi.org/10.5194/bg-16-2527-2019, URL https://bg.copernicus.org/articles/16/2527/2019/.

[38] Pietropolli G, Cossarini G, Manzoni L. GANs for integration of deterministic model and observations in marine ecosystem. In: Marreiros G, Martins B, Paiva A, Ribeiro B, Sardinha A, editors. Progress in artificial intelligence. Cham: Springer International Publishing; 2022, p. 452–63. http://dx.doi.org/10.1007/978-3-031-16474-3_37.

[39] Tedesco L, Vichi M, Thomas DN. Process studies on the ecological coupling between sea ice algae and phytoplankton. Ecol Model 2012;226:120–38. http://dx.doi.org/10.1016/j.ecolmodel.2011.11.011, URL https://www.sciencedirect.com/science/article/pii/S0304380011005400.

[40] Melaku Canu D, Ghermandi A, Nunes PA, Lazzari P, Cossarini G, Solidoro C. Estimating the value of carbon sequestration ecosystem services in the Mediterranean Sea: An ecological economics approach. Global Environ Change 2015;32:87–95. http://dx.doi.org/10.1016/j.gloenvcha.2015.02.008, URL https://linkinghub.elsevier.com/retrieve/pii/S0959378015000278.

[41] Wolf A, Swift JB, Swinney HL, Vastano JA. Determining Lyapunov exponents from a time series. Physica D 1985;16(3):285–317. http://dx.doi.org/10.1016/0167-2789(85)90011-9.

[42] Sankar S, Polimene L, Marin L, Menon N, Samuelsen A, Pastres R, et al. Sensitivity of the simulated oxygen minimum zone to biogeochemical processes at an oligotrophic site in the Arabian Sea. Ecol Model 2018;372:12–23. http://dx.doi.org/10.1016/j.ecolmodel.2018.01.016, URL https://www.sciencedirect.com/science/article/pii/S0304380018300395.

[43] Muratori S, Rinaldi S. Limit cycles and Hopf bifurcations in a Kolmogorov type system. Model Identif Control Nor Res Bull 1989;10(2):91–9. http://dx.doi.org/10.4173/mic.1989.2.3, URL http://www.mic-journal.no/ABS/MIC-1989-2-3.asp.

[44] Tilman D. Resource competition and community structure. (MPB-17), Volume 17. Princeton University Press; 1982, http://dx.doi.org/10.1515/9780691209654, URL https://www.degruyter.com/document/doi/10.1515/9780691209654/html.

[45] Martinez ND. Artifacts or attributes? Effects of resolution on the little rock lake food web. Ecol Monograph 1991;61(4):367–92. http://dx.doi.org/10.2307/2937047.

[46] Awender S, Wackerbauer R, Breed GA. Stability of generalized ecological-network models. Chaos 2021;31(2):023106. http://dx.doi.org/10.1063/5.0029934.

[47] Berryman AA, Stenseth NC, Isaev AS. Natural regulation of herbivorous forest insect populations. Oecologia 1987/01/01;71(2):174–84. http://dx.doi.org/10.1007/BF00377282.

[48] Rinaldi S, Muratori S, Kuznetsov Y. Multiple attractors, catastrophes and chaos in seasonally perturbed predator-prey communities. Bull Math Biol 1993;55(1):15–35. http://dx.doi.org/10.1007/BF02460293.

[49] Occhipinti G, Lazzari P. Stab-analyzer. 2023, http://dx.doi.org/10.5281/zenodo.7801214.